Polyhedron 52 (2013) 820–830

Contents lists available at SciVerse ScienceDirect

Polyhedron

journal homepage: www.elsevier.com/locate/poly

Exceptional thermal stability and high volatility in mid to late first row transition metal complexes containing carbohydrazide ligands

Mahesh C. Karunarathne [1], Thomas J. Knisley, Gabriel S. Tunstull, Mary Jane Heeg, Charles H. Winter *

Department of Chemistry, Wayne State University, Detroit, MI 48202, USA

ARTICLE INFO

Article history:
Available online 20 July 2012

Dedicated to Alfred Werner on the 100th Anniversary of his Nobel Prize in Chemistry in 1913.

Keywords:
Copper
Nickel
Cobalt
Iron
Manganese
Chromium
Coordination compound
Atomic layer deposition
Film growth precursor

ABSTRACT

Treatment of metal(II) halides (metal = Cu, Ni, Co, Fe, Mn, Cr) with the potassium salts of carbohydrazides L^1–L^6 afforded $Cu(L^1)_2$ (75%), $Cu(L^2)_2$ (51%), $Cu(L^3)_2$ (23%), $Co(L^1)_2$ (57%), $Cr(L^1)_2$ (62%), $Ni(L^1)_2$ (76%), $Ni(L^2)_2$ (62%), $Ni(L^3)_2$ (62%), $Ni(L^4)_2$ (13%), $Ni(L^5)_2$ (11%), $Ni(L^6)_2$ (29%), $[Fe(L^1)_2]_2$ (28%), and $[Mn(L^1)_2]_2$ (12%) as crystalline solids, where $L^1 = Me_2NN{=}C(tBu)O^-$, $L^2 = Me_2NN{=}C(iPr)O^-$, $L^3 = Me_2NN{=}C(Me)O^-$, $L^4 = (CH_2)_5NN{=}C(tBu)O^-$, $L^5 = (CH_2)_5NN{=}C(iPr)O^-$, and $L^6 = (CH_2)_5NN{=}C(Me)O^-$. These complexes were characterized by spectral and analytical techniques, and by X-ray crystal structure determinations for $Cu(L^1)_2$, $Co(L^1)_2$, $Cr(L^1)_2$, $Ni(L^1)_2$, and $[Fe(L^1)_2]_2$. $Cu(L^1)_2$, $Co(L^1)_2$, $Cr(L^1)_2$, and $Ni(L^1)_2$ exist as square planar, monomeric complexes, whereas $[Fe(L^1)_2]_2$ is a dimer. A combination of sublimation studies, thermal decomposition temperature determinations, and thermogravimetric/differential thermal analysis demonstrate that the Cu, Co, and Ni complexes $Cu(L^1)_2$, $Cu(L^2)_2$, $Co(L^1)_2$, $Ni(L^1)_2$, and $Ni(L^2)_2$ have the lowest sublimation temperatures and highest decomposition temperatures among the series. Additionally, these compounds have higher volatilities and thermal stabilities than commonly used ALD and CVD precursors. Hence, these new complexes have excellent properties for application as ALD precursors to Cu, Co, and Ni metal films.

1. Introduction

Thin films of first row transition metal elements have many important current and future applications. Copper (Cu) is the conductor of choice for interconnects in microelectronics devices, and is currently applied in the etched trenches and vias through a two-step process involving creation of a thin, conformal seed layer by physical vapor deposition, followed by electrodeposition fill [1]. However, Cu does not adhere well to SiO_2 surfaces, and the creation of a continuous seed layer is difficult. In response to this challenge, other metal seed layers for Cu metallization have been explored, including chromium (Cr), cobalt (Co), and ruthenium (Ru) [1,2]. Cu readily diffuses into SiO_2 layers and silicon (Si) substrates during the high temperatures encountered in microelectronics device fabrication. Therefore, a barrier between Cu and Si is required. This barrier must stop the diffusion of Cu at deposition temperatures long enough for manufacturing of the device, must be unreactive toward Cu and Si, and should exhibit good adhesion to Cu and Si. In addition, barriers in future devices should be $\leqslant$5 nm thick to reduce the electrical resistivity of the interconnect structure [1,3]. Materials that are currently under consideration as advanced barriers include TaN and WN_x (x = 0.5–1), as well as ternary compositions of these materials containing carbon or Si [2]. However, $\leqslant$5 nm thick layers of these nitride-based barrier materials may not serve as effective Cu diffusion barriers [1]. In response to this concern, considerable effort has been directed toward identification of alternative barrier materials. Very thin films ($\leqslant$5 nm) of transition metals such as manganese (Mn) [4], Cr [5,6], Ru [5], and others [6] have emerged as new Cu diffusion barrier materials. It has been recently demonstrated that annealing of a 150 nm thick 90/10 Cu/Mn alloy film on SiO_2 substrates at temperatures between 250 and 450 °C led to migration of the Mn atoms to the SiO_2 interface to form a segregated 2–8 nm $MnSi_xO_y$ layer between the SiO_2 and Cu layers [4]. Most significantly, this Mn-containing layer served as a Cu diffusion barrier for up to 100 h at 450 °C [4a] This work suggests that ultrathin Mn-based films can replace current nitride-based barriers in future microelectronics devices. There are other applications that require the growth of thin transition metal films. Magnetoresistive random access memory (MRAM) devices require thin, conformal layers of magnetic metals such as nickel (Ni), Co, or iron (Fe) [7]. In a recent report, 2.9–3.4 nm Cu nanocrystals grown by atomic layer deposition (ALD) on silica showed high catalytic activity for the water gas shift

* Corresponding author. Tel.: +1 313 577 5224; fax: +1 313 577 8289.
E-mail address: chw@chem.wayne.edu (C.H. Winter).
[1] Present address: Department of Chemistry, University of Sri Jayewardenepura, Nugegoda, Sri Lanka.

0277-5387/$ - see front matter © 2012 Elsevier Ltd. All rights reserved.
http://dx.doi.org/10.1016/j.poly.2012.07.034

reaction ($CO + H_2O \rightarrow H_2 + CO_2$) and performed better than platinum nanocrystals on silica supports [8]. Ni and nickel silicide (NiSi) are important contact materials in microelectronics devices [9].

The smallest microelectronics device dimensions are scheduled to reach 22 nm in 2012, and existing thin film deposition processes will soon not be able to provide the required level of thickness control and conformality, especially in high aspect ratio features [3,10]. The ALD technique is well suited for nanoscale film growth, since it produces inherently conformal films and affords angstrom-level film thickness control due to its self-limited growth mechanism [11]. In a typical ALD cycle, a metal precursor is carried in the vapor phase by an inert carrier gas into the reaction chamber, where it chemisorbs upon substrate surface reactive sites. Once all available surface reactive sites have been consumed, the surface is saturated, no further reactions can occur, and unreacted precursor and reaction byproducts are removed from the reactor with an inert gas purge. Next, a pulse of a second precursor vapor is passed over the substrate, which reacts with surface-adsorbed metal precursor to produce the desired thin film material. To conclude the deposition sequence, a second inert gas purge is then passed through the reactor to remove reaction byproducts and excess precursor. Under optimized deposition conditions, the growth rate per cycle remains constant, allowing the film thickness to be dependent upon the number of deposition cycles. ALD precursors must be thermally stable on the surface of the substrate at the deposition temperature, or else non-self-limited, chemical vapor deposition (CVD)-like growth occurs through precursor decomposition [11]. In addition, the metal precursor should be highly reactive toward a second precursor to afford the desired thin film material. Finally, ALD precursors should be as volatile as possible, since the minimum deposition temperature is often a few degrees higher than the precursor delivery temperature to avoid condensation in the reactor lines.

Transition metal thin films need to be deposited by ALD to meet future conformality and thickness uniformity requirements in microelectronics devices and nanotechnology. In addition, the metals should be deposited at the lowest possible temperatures (ideally $\leqslant 100$ °C) to afford the smallest surface roughnesses, promote facile nucleation, and give continuous films even at thicknesses of a few nanometers [12]. Thermal ALD is greatly preferred over plasma ALD, since the latter can lead to substrate damage from the highly reactive growth species and conformal coverage can be low due to surface radical recombination reactions that remove the reducing coreagents [13]. In general, ALD precursors for transition metal thin films should have thermal decomposition temperatures of $\geqslant 200$ °C and sublimation temperatures of $\leqslant 80$ °C at low pressures to allow a wide temperature window for film deposition. Additionally, transition metal ALD precursors must be highly reactive toward a reducing agent to afford high purity metal films.

ALD precursors processes for first row transition metal films are best developed for Cu. Direct Cu ALD processes include $CuL_2/ZnEt_2$ at 100–150 °C (L = $OCHMeCH_2NMe_2$, β-ketiminate, β-diketiminate) [12,14], $Cu(thd)_2/H_2$ at 190–260 °C (thd = 2,2,6,6-tetramethyl-3,5-heptanedionate) [15], $[Cu(sBuNCMeNsBu)]_2/H_2$ at 150–250 °C [16–18], $Cu(hfac)_2$/alcohol at 300 °C (hfac = 1,1,1,5,5,5-hexafluoro-3,5-pentanedionate) [19], $CuCl/H_2$ at 360–410 °C [20], and CuCl/Zn at 440–500 °C [21]. ALD Cu growth was claimed from a Cu(I) β-diketiminate precursor and diethylsilane [22], but a later study showed that this process proceeds by a pulsed chemical vapor deposition (CVD) mechanism [23]. Indirect routes to Cu films include reduction of ALD CuO by isopropanol [24], reduction of ALD Cu_3N with H_2 [25], and reduction of ALD Cu_2O by formic acid in conjunction with a ruthenium seed layer [26]. Plasma-based ALD processes include $Cu(acac)_2$/hydrogen plasma (acac = 2,4-pentanedionate) [27] and $Cu(OCHMeCH_2NMe_2)_2$/hydrogen plasma [28]. Problems with existing Cu ALD processes include high growth temperatures, lack of self-limited growth in many systems due to precursor thermal decomposition, low reactivity of the Cu precursors toward the reducing co-reagents, incorporation of zinc in processes using $ZnEt_2$, and substrate damage and low conformal coverage in plasma processes. We have recently reported a 3-step Cu ALD process that entails the use of $Cu(OCHMeCH_2NMe_2)_2$, formic acid, and hydrazine [29]. This process affords self-limited growth between 100 and 170 °C with a high growth rate of 0.50 Å/cycle. However, self-limited growth is lost above 170 °C due to thermal decomposition of $Cu(OCHMeCH_2NMe_2)_2$. ALD precursors for Ni metal growth have contained amidinate, alkoxide, or cyclopentadienyl ligands, and reducing co-reagents have included ammonia plasma, hydrogen plasma, and molecular hydrogen [9,16]. Growth of Co metal films by ALD has used precursors containing cyclopentadienyl, amidinate, and carbonyl ligands [30]. The associated reducing co-reagents were dimethylhydrazine, ammonia plasma, hydrogen plasma, and nitrogen plasma. ALD growth of Fe metal on aerogels was reported [31], but details were not given. Mn and Cr metal films have not been grown by thermal ALD, but a plasma ALD process for Cu/Mn alloy films was recently reported using a Mn β-diketonate precursor [32]. Existing ALD precursors for Cu, Ni, and Co generally suffer from low thermal stability, low reactivity toward reducing agents, or a combination of both [9,16,30–32].

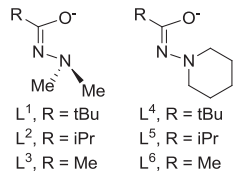

Chart 1. Chemical structures of L^1–L^6.

Herein, we report the synthesis, structure, and precursor properties of a series of Cu, Ni, Co, Fe, Mn, and Cr complexes that contain carbohydrazide ligands chosen from L^1 to L^6 (Chart 1). The Cu, Ni, and Co complexes are highly volatile, have very high solid state decomposition temperatures, and thus have promising properties for use as ALD precursors. Carbohydrazide ligands have previously been widely used in Si [33] and Ge [34] compounds. However, the coordination chemistry of these ligands with transition metals has been limited to a few copper complexes [35], a nickel complex [35a], and a platinum complex [36].

2. Results and discussion

2.1. Synthetic aspects

The carbohydrazine ligand precursors L^1H–L^6H (Chart 1) were prepared and characterized as described in Section 4 by treatment of the carboxylic acid chloride with 1,1-dimethylhydrazine or 1-aminopiperidine in the presence of triethylamine. Treatment of anhydrous copper(II) chloride with two equivalents of KL^1, KL^2, or KL^3 (prepared *in situ* from L^1H–L^3H and potassium hydride) in tetrahydrofuran afforded $Cu(L^1)_2$ (**1**, 75%), $Cu(L^2)_2$ (**2**, 51%), and $Cu(L^3)_2$ (**3**, 23%), respectively, as maroon crystals upon sublimation of the crude products at 70–80 °C/0.05 Torr (Eq. (1)). Similar treatment of cobalt(II) chloride or chromium(II) chloride with KL^1 afforded $Co(L^1)_2$ (**4**, 57%) and $Cr(L^1)_2$ (**5**, 62%) as red and orange crystalline solids, respectively. Treatment of $NiCl_2{\cdot}CH_3CN$ with two equivalents of KL^1–KL^6 afforded $Ni(L^1)_2$ (**6**, 76%), $Ni(L^2)_2$ (**7**, 62%), $Ni(L^3)_2$ (**8**, 62%), $Ni(L^4)_2$ (**9**, 13%), $Ni(L^5)_2$ (**10**, 11%), and $Ni(L^6)_2$ (**11**, 29%) as orange crystals upon sublimation between 70 and 80 °C/0.05 Torr (Eq. (2)). Treatment of anhydrous iron(II)

chloride or manganese(II) bromide with two equivalents of KL^1 in tetrahydrofuran afforded the dinuclear complexes $[Fe(L^1)_2]_2$ (**12**, 28%) and $[Mn(L^1)_2]_2$ (**13**, 12%), respectively (Eq. (3)). Similar treatment of cobalt(II), chromium(II), iron(II), or manganese(II) halides with the less sterically encumbered KL^2 or KL^3 did not generate isolable products or gave very low yields.

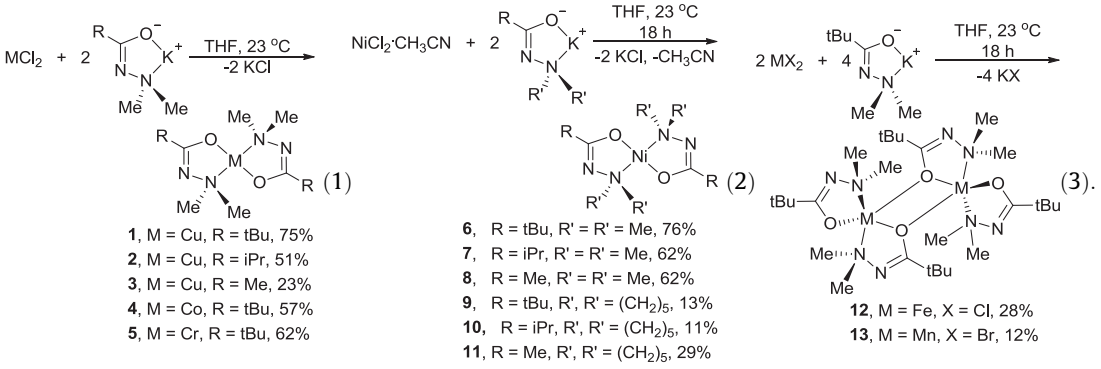

The structural assignments for **1**–**13** are based upon spectral and analytical data. In addition, X-ray crystal structure determinations were carried out for **1**, **4**, **5**, **6**, and **12**. The ^1H NMR spectra of **1**–**5**, **12**, and **13** show extremely broad resonances due to their paramagnetic nature, while the corresponding spectra of **6**–**11** in benzene-d_6 exhibit sharp signals for the ligand substituents, which can be attributed to spin-paired, diamagnetic d^8 Ni(II) centers. The solid state magnetic moment (μ_{eff}) values of **1**–**3** range between 1.51 and 1.69 BM, which are close to the spin only magnetic moment expected for a d^9 Cu(II) center with one unpaired electron (μ_{eff} = 1.73 BM). Complex **4**, which has a d^7 electron configuration and would be expected to have a magnetic moment value close to 1.73 BM if low-spin or 3.87 BM if high-spin, exhibited magnetic moment values of 2.17 BM both in the solid state and in benzene solution. This value suggests a low spin configuration. Complex **5** has solid state and solution magnetic moments of 4.84 and 5.04 BM, respectively, which are close to the spin only magnetic moment expected for a high-spin d^4 Cr(II) center with four unpaired electrons (μ_{eff} = 4.90 BM). Complexes **12** and **13** have solution magnetic moments of 4.55 and 5.47 BM, respectively. These values are close to those expected for four and five unpaired electrons (μ_{eff} = 4.90, 5.92 BM), respectively, and may indicate the formation of tetrahedral, monomeric structures for **12** and **13** in benzene. For comparison, the solid state magnetic moments for **12** (7.99 BM) and **13** (9.62 BM) were much higher than in solution.

2.2. Structural aspects

The crystal structures of **1**, **4**, **5**, **6**, and **12** were obtained to establish the geometries about the metal centers and to assess the bonding modes of the carbohydrazide ligands. Experimental crystallographic data are summarized in Table 1 and selected bond lengths and angles are presented in Tables 2 and 3. Perspective views of **1**, **4**, **5**, **6**, and **12** are given in Figs. 1–5. A low precision X-ray crystal structure determination of **13** demonstrated a dinuclear structure similar to that of **12**. The spectral data of **2**, **3**, **7**, **8**, **9**, **10**, and **11** are similar to those of the structurally characterized complexes **1**, **4**, **5**, and **6**, which suggest similar, square planar monomers for the former group of compounds.

Table 1
Crystal data and data collection parameters for **1**, **4**, **5**, **6**, and **12**.

	1	**4**	**5**	**6**	**12**
Formula	$C_{14}H_{30}CuN_4O_2$	$C_{14}H_{30}CoN_4O_2$	$C_{14}H_{30}CrN_4O_2$	$C_{14}H_{30}N_4NiO_2$	$C_{28}H_{60}Fe_2N_8O_4$
FW	349.96	345.35	338.42	345.13	684.54
Space group	$P2_1/n$	$P2_1/n$	$P2_1/n$	$P2_1/n$	$P\bar{1}$
a (Å)	5.6414(2)	5.65930(10)	5.6015(2)	5.6745(5)	11.3304(4)
b (Å)	8.8780(3)	8.8040(2)	9.0727(4)	8.7346(7)	12.6325(5)
c (Å)	17.9543(5)	18.0989(5)	17.5995(7)	18.2007(13)	13.4921(6)
α (°)					81.6893
β (°)	94.233010	95.218010	91.6822	95.3795	73.5693
γ (°)					89.3823
V (Å^3)	896.78(5)	898.03(4)	894.03(6)	898.14(12)	1831.90(13)
Z	2	2	2	2	2
T (K)	100(2)	100(2)	100(2)	100(2)	100(2)
λ (Å)	0.71073	0.71073	0.71073	0.71073	0.71073
ρ_{calc} (g cm^{-3})	1.296	1.277	1.257	1.276	1.241
μ (mm^{-1})	1.227	0.965	0.649	1.090	0.833
$R(F)$ (%)	2.47	2.60	2.95	5.89	9.76
$Rw(F)$ (%)	6.46	6.07	7.21	16.28	26.78

$R(F) = \sum||F_o| - |F_c||/\sum|F_o|$; $Rw(F) = [\sum w(F_o^2 - F_c^2)^2/\sum w(F_o^2)^2]^{1/2}$ for $I > 2\sigma(I)$.

Table 2
Selected bond lengths (Å) and angles (°) for **1**, **4**, **5**, and **6**.

	1	4	5	6
M–O	1.9023(7)	1.8463(8)	1.9629(6)	1.840(1)
M–N	1.9924(8)	1.938(1)	2.0910(7)	1.906(2)
N–N	1.468(1)	1.478(1)	1.477(1)	1.479(3)
Core N–C	1.298(1)	1.291(2)	1.297(1)	1.291(3)
N–CH_3	1.478(1)	1.479(2)	1.475(1)	1.476(4)
	1.478(1)	1.480(2)	1.480(1)	1.490(3)
C–O	1.310(1)	1.322(1)	1.311(1)	1.315(3)
N–M–O	96.75(3)	95.49(4)	99.99(3)	94.58(8)
	83.25(3)	84.51(4)	80.01(3)	85.42(8)

Complexes **1**, **4**, **5**, and **6** have four-coordinate monomeric structures with square planar geometry around the metal centers (Figs. 1–4). All molecules have an inversion center located on the metal atom. The carbohydrazide ligands are coordinated in a chelating κ^2-fashion through the carbonyl oxygen atom and dimethylamino nitrogen atom. The carbohydrazide ligand core C–N bond lengths range between 1.291 and 1.298 Å, which are in between the distances expected for C–N single (1.46 Å) and C=N double bonds (1.21 Å) [37]. The oxygen and nitrogen donor atoms in the two ligands are mutually trans, with N–M–N′ and O–M–O′ angles of 180.00°. The intraligand N–M–O angles range between 80.01(3)° and 85.42(8)°, and the related interligand angles lie between

Table 3
Selected bond lengths (Å) and angles (°) for **12**.

Fe1–O1	1.954(4)
Fe1–O2	2.066(3)
Fe1–O3	2.111(3)
Fe2–O2	2.111(3)
Fe2–O3	2.061(3)
Fe2–O4	1.964(4)
Fe1–N1	2.197(4)
Fe1–N5	2.198(5)
Fe2–N3	2.235(5)
Fe2–N7	2.127(5)
N1–N2	1.482(6)
N3–N4	1.468(7)
N5–N6	1.462(6)
N7–N8	1.489(7)
N2–C1	1.305(7)
N4–C8	1.305(7)
N6–C15	1.301(7)
N8–C22	1.331(8)
C1–O1	1.300(6)
C8–O2	1.361(6)
C15–O3	1.340(6)
C22–O4	1.257(7)
O1–Fe1–O2	108.0(2)
O1–Fe1–O3	174.6(1)
O1–Fe1–N1	77.9(2)
O1–Fe1–N5	102.0(2)
O2–Fe1–O3	77.4(1)
O2–Fe1–N1	124.5(2)
O2–Fe1–N5	127.4(2)
O3–Fe1–N1	99.8(2)
O3–Fe1–N5	73.6(2)
N1–Fe1–N5	103.2(2)
O2–Fe2–O3	77.4(1)
O2–Fe2–O4	171.8(2)
O2–Fe2–N3	125.2(2)
O2–Fe2–N7	102.2(2)
O3–Fe2–O4	108.5(2)
O3–Fe2–N3	74.3(2)
O3–Fe2–N7	125.3(2)
O4–Fe2–N3	97.5(2)
O4–Fe2–N7	79.2(2)
N3–Fe2–N7	106.2(2)
Fe1–O2–Fe2	102.5(1)
Fe1–O3–Fe2	102.7(1)

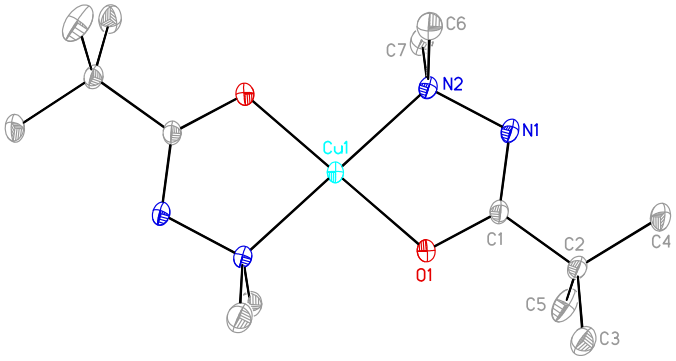

Fig. 1. Perspective view of **1** with thermal ellipsoids at the 50% probability level.

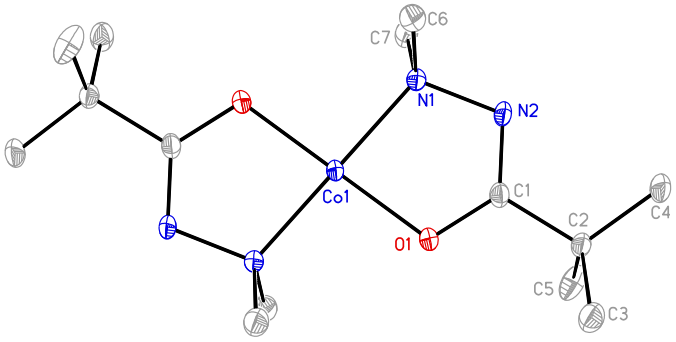

Fig. 2. Perspective view of **4** with thermal ellipsoids at the 50% probability level.

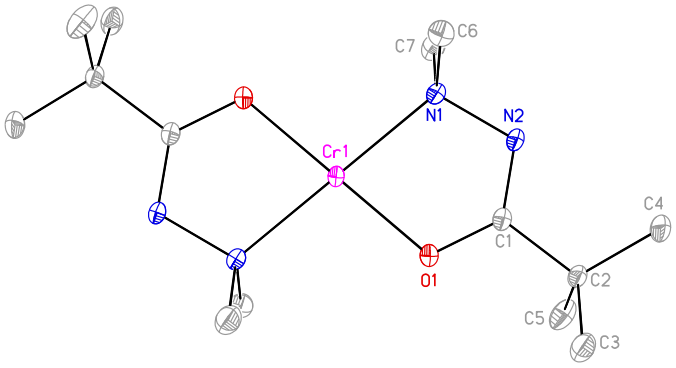

Fig. 3. Perspective view of **5** with thermal ellipsoids at the 50% probability level.

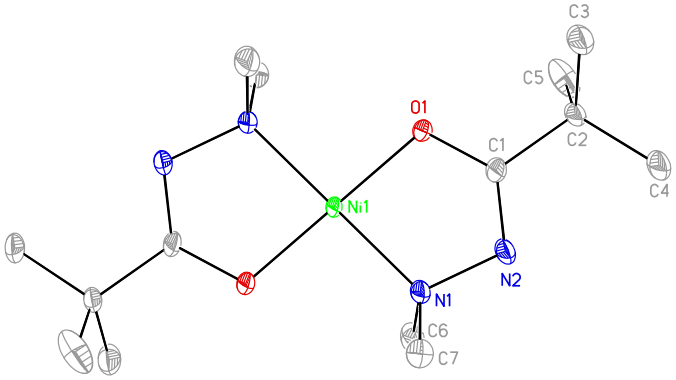

Fig. 4. Perspective view of **6** with thermal ellipsoids at the 50% probability level.

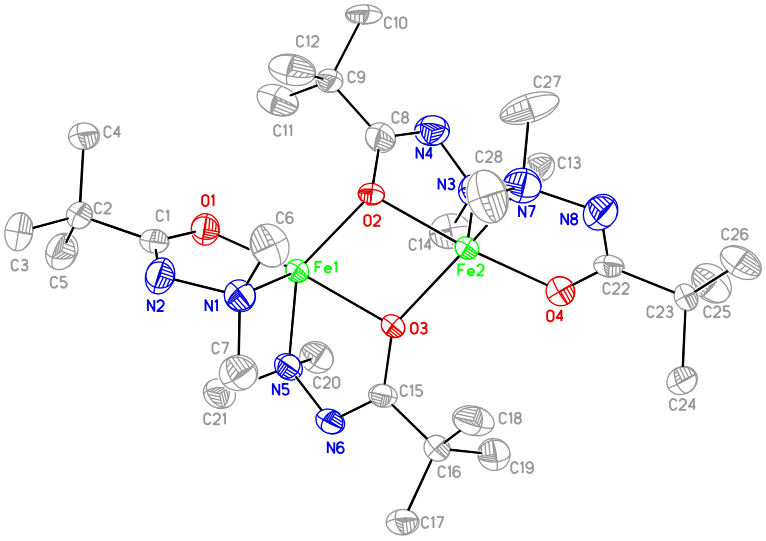

Fig. 5. Perspective view of **12** with thermal ellipsoids at the 50% probability level.

Table 4
Sublimation temperature, melting point, solid state decomposition temperature, percent recovery, and percent nonvolatile residue for **1**–**13**.

Complex	Sublimation temperature (°C/ 0.05 Torr)	Melting point (°C)	Solid state decomposition temperature (°C)	% recovery	% nonvolatile residue
1	70	137–139	255	>99	0.0
2	75	118–121	247	>99	0.0
3	80	184–187	225	98.1	0.5
4	75	137–140	245	97.7	0.0
5	non-volatile	143–146	150	–	–
6	70	140–142	323–325	>99	0.0
7	80	125–128	317	>99	0.0
8	80	164–166	320	>99	0.0
9	155	203–205	282	95.8	0.8
10	110	115–117	248	97.6	0.9
11	150	230–232	273	96.9	0.2
12	non-volatile	155–157	160	–	–
13	non-volatile	92–94	96	–	–

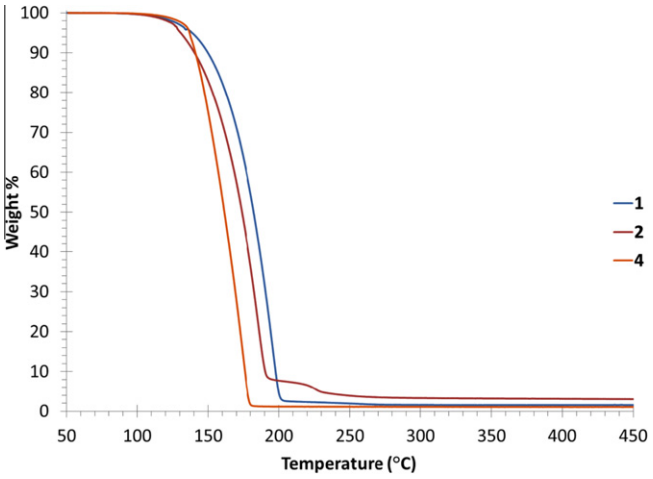

Fig. 6. TGA plots of complexes **1**, **2**, and **4**.

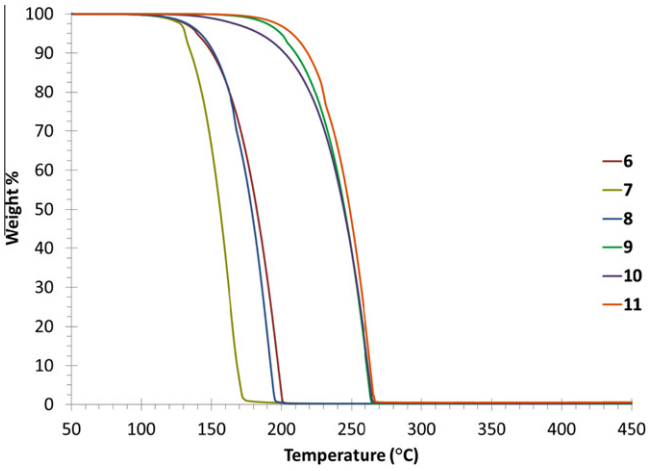

Fig. 7. TGA plots of Ni complexes **6**–**11**.

94.58(8)° and 99.99(3)°. The two nitrogen atoms, two oxygen atoms, and the metal ion are planar to <0.002 Å. The metal-nitrogen distances (**1**, 1.9924(8); **4**, 1.938(1); **5**, 2.0910(7); **6**, 1.906(2) Å) are uniformly longer than the metal–oxygen distances (**1**, 1.9023(7); **4**, 1.8463(8); **5**, 1.9629(6); **6**, 1.840(1) Å), consistent with neutral dimethylamino and anionic oxygen donor atoms, respectively. A square planar Cu(II) complex, $Cu(OC(O\text{-}2,4\text{-}Cl_2C_6H_3)=NNMe_2)_2$ [35a], with an inner coordination sphere similar to that of **1**, has Cu–O distances of 1.901(3) and 1.910(3) Å and Cu–N distances of 1.985(3) and 2.001(3) Å. These values are very close to those of **1**. The square planar β-ketiminate complexes $Co(OC(CH_2C_6H_5)CHC(CH_2C_6H_5)NCH_2CH_2NC(CH_2C_6H_5)CHC(CH_2C_6H_5)O)$ (Co–O 1.852(1), 1.854(1); Co–N 1.858(1), 1.862(1) Å) [38], $Ni(OCMeCHCMeN(2,6\text{-}iPr_2C_6H_3))_2$ (Ni–O, 1.818(1); Ni–N, 1.919(1) Å) [39], and $Cr(OCMeCHCMeN(C_6H_{11}))_2$ (Cr–O 1.971(2), 1.977(2); Cr–N 2.085(3), 2.091(3) Å) [40] have metal–oxygen and metal–nitrogen bond lengths that are very similar to those of **4**–**6**.

Compound **12** exists as a dinuclear complex in which each iron atom is bonded to the nitrogen and oxygen donor atoms of one carbohydrazide ligand in a terminal κ^2-fashion and to one nitrogen and two oxygen atoms of two bridging carbohydrazide ligands with $\mu\text{-}\kappa^1\text{:}\kappa^2$-interactions (Fig. 5). The carbohydrazide ligand core C–N bond lengths range from 1.301(7) to 1.331(8) Å, which are similar to slightly longer than those of **1**, **4**, **5**, and **6**. The geometry around each iron center can be approximated as distorted trigonal

bipyramidal with two oxygen atoms from one κ^2 and one μ-κ^1:κ^2 ligand occupying the axial positions while two nitrogen atoms from one κ^2 and one μ-κ^1:κ^2 ligand and one oxygen atom from the other μ-κ^1:κ^2 ligand form the equatorial plane. The calculated index of trigonality, $\tau = 0.780$, agrees well with this geometry assignment [41]. Not surprisingly, the Fe–O bond lengths for the terminal ligands (1.954(4), 1.964(4) Å) are shorter than those associated with the bridging ligands (2.061(3), 2.066(3), 2.111(3), 2.111(3) Å). Additionally, the iron–oxygen distances within the Fe_2O_2 core are slightly asymmetric. The N–Fe–O bite angles associated with the bridging ligands (73.62(15)° and 74.28(16)°) are smaller compared to the corresponding angles of the terminal ligands (77.88(16)° and 79.21(19)°). These values are also slightly smaller than those observed in **1**, **4**, **5**, and **6**. As a result of the strain of the molecule, the carbohydrazide ligand planes marginally deviate from planarity, which can be defined by the N–N–C–O torsion angles (terminal, 3.7(8)°, −2.8(9)°; bridging, 6.3(9)°, 3.2(7)°). All other bond lengths and angles are similar to those of **1**, **4**, **5**, and **6**.

2.3. Evaluation of thermal stability and volatility

The preparative sublimation and decomposition temperature data for **1**–**13** are summarized in Table 4. The Cu, Ni, and Co complexes are volatile, and sublime at temperatures between 70 and 80 °C at 0.05 Torr. The Cr (**5**) and Fe (**12**) complexes undergo simultaneous decomposition during sublimation, whereas the Mn complex **13** decomposes without sublimation. In preparative sublimation experiments, 0.5–1.0 g samples of **1**–**4** and **6**–**11** sublimed within 4 h with no detectable residue and near-quantitative recoveries. To determine decomposition ranges, a 2–3 mg sample of each complex was sealed in melting point tubes under argon at atmospheric pressure and was heated at the rate of 5 °C/min. The samples sublimed out of the heated portion of the tube between 240 and 285 °C, and there was no residue or evidence of any thermal decomposition when the tubes were inspected under a microscope. Accurate thermal decomposition temperatures in the condensed phase reported in Table 4 were measured by restricting the samples to the hot region of the melting point apparatus by using sealed melting point tubes that were no more than 8 mm long. The Ni complexes **6**–**11** are extremely thermally stable and show no evidence for thermal decomposition at temperatures below 248 °C. The analogous Cu and Co complexes **1** and **4** are stable up to 255 and 245 °C, respectively. Notably, **1**, **2**, **4**, **6**, **7**, and **10** melt between 117 and 142 °C and exhibit a remarkably wide span of temperatures (105–190 °C) after melting and prior to thermal decomposition. Liquid precursors are desirable, since they avoid the particles that can be generated with solid precursors [11].

Simultaneous thermogravimetric analyses (TGA) and differential thermal analyses (DTA) were performed on **1**, **2**, **4**, and **6**–**11** to understand their volatilities and thermal stabilities. Complex **3** was too air sensitive to obtain these analyses, whereas **5** decomposed upon sublimation. Selected data are shown in Figs. 6 and 7. Complexes **1**, **2**, **4**, and **6**–**11** have similar TGA traces with single-step weight losses occurring between 150 and 250 °C. The final percent residues upon reaching 450 °C were all $\leqslant$3.0%. These results further demonstrate the volatility and high thermal stabilities of **1**, **2**, **4**, and **6**–**11**. Each DTA plot of **1**, **2**, **4**, and **6**–**11** revealed two endotherms associated with the melting and evaporation points. Exothermic peaks associated with thermal decomposition were not observed due to the complete evaporation at temperatures lower than the decomposition points.

The Cu, Co, and Ni complexes **1**–**4** and **6**–**11** allow insights into how the ligand substituents affect volatility. The dimethylhydrazine-derived complexes **1**–**4** and **6**–**8** sublime with quantitative recovery between 70 and 80 °C/0.05 Torr. The alkoxide complex $Cu(OCHMeCH_2NMe_2)_2$ [29,42] is widely used as a Cu CVD and ALD precursor. This complex sublimes at 90 °C/0.05 Torr [29], so **1**–**4** and **6**–**8** are slightly more volatile than this benchmark Cu precursor. The low sublimation temperatures of **1**–**4** and **6**–**8** should allow low temperature ALD growth of Cu, Co, and Ni films (probably < 100 °C), in concert with an appropriate co-reagent. Complexes **1**–**4** and **6**–**11** also afford insights into how the various substituents affect thermal decomposition temperatures. These decomposition temperatures are a good estimate of the upper temperature limit for self-limited ALD growth [29], and hence provide valuable information. The thermal stability of the Cu precursors decreases in the order **1** > **2** > **3**, which follows decreasing ligand steric bulk. The larger alkyl groups may decrease intermolecular decomposition reactions, and thus increase thermal stability. The decomposition points of **1**–**3** (255–225 °C) are considerably higher than that of $Cu(OCHMeCH_2NMe_2)_2$ (185–188 °C) [29], which suggests that self-limited Cu ALD with these precursors may occur over a wider temperature range than is possible with $Cu(OCHMeCH_2NMe_2)_2$ (100–170 °C) [29]. The TGA data suggest that the isopropyl-substituted Cu complex **2** is slightly more volatile than the *tert*-butyl-substituted Cu complex **1**. The Co complex **4** has a similar sublimation temperature and very similar TGA behavior as the isostructural complex **1**. Among the Ni complexes **6**–**11**, the dimethylamino-containing complexes **6**–**8** are significantly more volatile than the piperidine-containing complexes **9**–**11**. Complexes **9**–**11** have similar volatilities irrespective of the ligand core carbon-bound alkyl group size, but the isopropyl-substituted complex **7** is more volatile than the *tert*-butyl- and methyl-substituted complexes **6** and **8**. The volatility differences between **9**–**11** and **6**–**8** can be ascribed to the higher molecular weights of **9**–**11**, but the evaporation rate trends of **6**–**8** are more subtle. The asymmetric isopropyl groups in **2** and **7** may lead to less efficient crystal packing, lower lattice energy, and higher volatility, relative to **1**, **3**, **6** and **8**. Overall, the Cu, Co, and Ni complexes **1**, **2**, **4**, **6**, and **7** have the highest volatilities and highest decomposition temperatures among **1**–**13**. These complexes have excellent properties for application as ALD precursors to Cu, Co, and Ni metal films. Film deposition studies of these precursors will be published separately. Finally, the carbohydrazide ligands do not have sufficient steric bulk to afford monomeric Fe and Mn complexes. Instead, dinuclear complexes result that have poor volatilities and low solid state decomposition temperatures.

3. Conclusions

We have prepared a series of Cu, Ni, Co, Fe, Mn, and Cr complexes **1**–**13** containing carbohydrazide ligands selected from L^1 to L^6. These complexes adopt monomeric, square planar structures for Cu, Ni, Co, and Cr, and dinuclear structures for Mn and Fe. A combination of sublimation studies, thermal decomposition determinations, and TGA/DTA demonstrate that the Cu, Co, and Ni complexes **1**, **2**, **4**, **6**, and **7** have the highest volatilities and highest decomposition temperatures among **1**–**13**. Additionally, these compounds have higher volatilities and thermal stabilities than commonly used ALD and CVD precursors. Hence, the new complexes have excellent properties for application as ALD precursors to Cu, Co, and Ni metal films. The Cr complex **5**, Fe complex **12**, and Mn complex **13** are nonvolatile.

4. Experimental

4.1. General considerations

All metal–organic reactions were performed under argon using standard glove box and Schlenk line techniques. Tetrahydrofuran

and diethyl ether were freshly distilled from sodium benzophenone ketyl, toluene was distilled from sodium, and hexane was distilled from P_2O_5. All carboxylic acid chlorides, triethylamine, and 1-aminopiperidine were purchased from Acros Organics. Anhydrous transition metal chlorides ($CrCl_2$, $MnCl_2$, $FeCl_2$, $CoCl_2$, $NiCl_2$, and $CuCl_2$) were obtained from Strem Chemicals and were used as received. Potassium hydride (30 wt% dispersion in mineral oil; washed with hexane before use) and 1,1-dimethylhydrazine were purchased from Sigma–Aldrich. $NiCl_2{\cdot}CH_3CN$ was prepared according to a published procedure [43].

^1H and $^{13}C\{^1H\}$ NMR spectra were obtained at 300 and 75 MHz in benzene-d_6. Infrared spectra were obtained as neat liquids, KBr pellets, or Nujol mulls. Elemental analyses were performed by Midwest Microlab, Indianapolis, IN. Melting points were obtained on a Thermo Scientific Mel-Temp 3.0 digital melting point apparatus and are uncorrected. Magnetic susceptibility measurements in benzene solution and in the solid state were determined using the Evans method with a 500 MHz NMR spectrometer, and a Johnson–Matthey magnetic susceptibility balance, respectively. Thermogravimetric analysis (TGA) was conducted on a TA Instruments SDT 2960 TGA/DTA system between 50 and 450 °C, using nitrogen as the flow gas with a heating rate of 10 °C/min. Solution magnetic moments were measured in benzene solutions using the Evans method [44].

4.2. Preparation of N′,N′-dimethylpivalohydrazine (L^1H)

A 500-mL round bottomed flask was charged with 1,1-dimethylhydrazine (3.88 mL, 50 mmol), triethylamine (7.52 mL, 53 mmol), and diethyl ether (250 mL). To this stirred solution at 0 °C was slowly added pivaloyl chloride (6.28 mL, 50 mmol). The resultant white suspension was stirred at ambient temperature for 18 h. This suspension was then filtered through a sintered glass funnel to afford a colorless solution. The volatile components were then removed and the resultant white solid was sublimed at 65 °C/0.05 Torr to afford L^1H as colorless crystals (6.95 g, 96%): mp 120–122 °C; IR (KBr pellet, cm^{-1}) 1650 (ν_{CO}, s); ^1H NMR (C_6D_6, 23 °C, δ) 6.84 (br s, 1H, N*H*), 2.61 (s, 6H, N(CH_3)$_2$), 1.02 (s, 9H, C(CH_3)$_3$); $^{13}C\{^1H\}$ NMR (C_6D_6, 23 °C, ppm) 175.95 (s, *C*=O), 45.68 (s, N(CH_3)$_2$), 38.08 (s, *C*(CH_3)$_3$), 27.43 (s, C(CH_3)$_3$); ESI-HRMS: calcd for $C_7H_{16}N_2ONa$ ([M+Na]$^+$) 167.1160, found 167.1152.

4.3. Preparation of N′,N′-dimethylisobutyrohydrazine (L^2H)

In a fashion similar to the preparation of L^1H, treatment of a diethyl ether (250 mL) solution of 1,1-dimethylhydrazine (3.88 mL, 50 mmol) and triethylamine (7.52 mL, 53 mmol) with isobutyryl chloride (5.39 mL, 50 mmol) afforded L^2H as colorless crystals upon crystallization from Et_2O and subsequent sublimation at 60 °C/0.05 Torr (6.12 g, 94%): mp 94–96 °C (lit. mp [45] 89–90 °C); IR (KBr pellet, cm^{-1}) 1656 (ν_{CO}, s); ^1H NMR (C_6D_6, 23 °C, δ) major isomer, 8.22 (br s, 1H, N*H*), 3.19 (septet, 1H, C*H*(CH_3)$_2$), 2.17 (s, 6H, N(CH_3)$_2$), 1.18 (d, 6H, CH(CH_3)$_2$), minor isomer, 7.67 (br s, 1H, N*H*), 2.60 (s, 6H, N(CH_3)$_2$), 2.16 (septet, 1H, C*H*(CH_3)$_2$), 1.10 (d, 6H, CH(CH_3)$_2$); $^{13}C\{^1H\}$ NMR (C_6D_6, 23 °C, ppm) major isomer, 180.17 (s, *C*=O), 48.25 (s, N(CH_3)$_2$), 29.66 (s, *C*H(CH_3)$_2$), 19.47 (s, CH(*C*H$_3$)$_2$), minor isomer, 174.95 (s, *C*=O), 46.01 (s, N(*C*H$_3$)$_2$), 33.73 (s, *C*H(CH_3)$_2$), 19.73 (s, CH(CH_3)$_2$).

4.4. Preparation of N′,N′-dimethylacetohydrazine (L^3H)

A 500-mL round bottom flask was charged with 1,1-dimethylhydrazine (3.88 mL, 50 mmol), triethylamine (7.52 mL, 53 mmol), and diethyl ether (250 mL). To this stirred solution at 0 °C was slowly added acetyl chloride (3.63 mL, 50 mmol). The resultant white suspension was stirred at ambient temperature for 18 h. This suspension was then filtered through a sintered glass funnel to afford a colorless solution. The volatile components were then removed and the resultant pale yellow oil was distilled at 70 °C/0.05 Torr (lit. bp 98 °C/16 Torr [46]) to afford L^3H as a colorless liquid (4.34 g, 85%): IR (neat liquid, cm^{-1}) 1660 (ν_{CO}, s); ^1H NMR (C_6D_6, 23 °C, δ) major isomer, 8.61 (br s, 1H, N*H*), 2.18 (s, 6H, N(CH_3)$_2$), 2.01 (s, 3H, CH_3), minor isomer, 8.01 (br s, 1H, N*H*), 2.59 (s, 6H, N(CH_3)$_2$), 1.74 (s, 3H, CH_3); $^{13}C\{^1H\}$ NMR (C_6D_6, 23 °C, ppm) major isomer, 174.08 (s, *C*=O), 47.83 (s, N(CH_3)$_2$), 19.63 (s, CH_3), minor isomer, 167.91 (s, *C*=O), 46.13 (s, N(CH_3)$_2$), 21.53 (s, CH_3).

4.5. Preparation of N-(1-piperidinyl)pivalamide (L^4H)

A 100 mL Schlenk flask was charged with 1-aminopiperidine (2.156 mL, 19.97 mmol), triethylamine (2.782 mL, 19.97 mmol), and diethyl ether (300 mL). Pivaloyl chloride (1.889 mL, 10.25 mmol) was slowly added to the stirred solution at 0 °C. The resultant white solution was stirred at ambient temperature for 17 h. The solution was filtered through a coarse glass funnel to afford a colorless solution. Volatile components were subsequently removed and the resultant white powder was collected and sublimed at 111 °C/0.05 Torr to afford L^4H as colorless crystals (1.889 g, 51.3%): mp 141–143 °C; IR 1651 (ν_{CO}, s); ^1H NMR ($CDCl_3$, 23 °C, δ) 6.30 (br s, 1H, N*H*), 2.71 (t, 4H, N(CH_2)$_2$), 1.67 (p, 4H, CH_2), 1.37 (p, 2H, CH_2), 1.16 (s, 9H, (CH_3)$_3$); $^{13}C\{^1H\}$($CDCl_3$, 23 °C, ppm) 175.27 (s, *C*=O), 56.70 (s, *C*H$_2$), 38.06 (s, *C*(CH_3)$_3$), 27.48 (s, C(*C*H$_3$)$_3$), 25.37 (s, *C*H$_2$), 23.29 (s, *C*H$_2$).

4.6. Preparation of N-(1-piperidinyl)isobutyramide (L^5H)

In a fashion similar to the preparation of L^4H, treatment of a diethyl ether (30 mL) solution of 1-aminopiperidine (2.155 mL, 19.97 mmol) and triethylamine (2.784 mL, 19.97 mmol) with isobutyryl chloride (2.092 mL, 19.97 mmol) afforded colorless crystals of L^5H after workup (1.342 g, 39.5%): mp 127–129 °C; IR 1655 (ν_{CO}, s); ^1H NMR ($CDCl_3$, 23 °C, δ) major isomer, 6.03 (br s, 1H, N*H*), 3.09 (septet, 1H, CH(CH_3)$_2$), 2.70 (t, 4H, N(CH_2)$_2$), 2.20 (p, 4H, CH_2), 1.65 (p, 2H, CH_2), 1.70 (s, 6H CH(*C*H$_3$)$_2$), minor isomer, 6.15 (br s, 1H, NH), 3.0 (t, 4H, N(CH_2)$_2$), 1.38 (p, 4H, CH_2), 1.36 (p, 2H, CH_2), 1.09 (s, 6H, C(CH_3)$_2$, minor isomer, 3.09 (septet, 1H, C*H*(CH_3)$_2$), 2.70 (t, 4H, N(CH_2)$_2$), 1.38 (p, 4H, CH_2), 1.36 (p, 2H, CH_2) 1.86 (br s, 1H, O*H*), 1.07 (s, 6H, CH(*C*H$_3$)$_2$); $^{13}C\{^1H\}$($CDCl_3$, 23 °C, ppm) major isomer, 172.25 (s, *C*=O), 58.35 (s, N(*C*H$_2$)$_2$), 34.23 (s, *C*H$_2$), 25.59 (s, *C*H$_2$), 25.26 (s, *C*H$_2$), 19.03 (s, CH(*C*H$_3$)$_2$), minor isomer, 176.59 (s, *C*=O) 56.96 (s, N(*C*H$_2$)$_2$, 25.49 (s, *C*H$_2$), 23.23 (s, *C*H$_2$), minor isomer, 56.93 (s, N(*C*H$_2$), 29.84 (s, *C*H(CH$_3$)$_2$), 25.59 (s, *C*H$_2$), 22.98 (s, *C*H$_2$), 18.80 (s, C(*C*H$_3$)$_2$).

4.7. Preparation of N-(1-piperidinyl)acetamide (L^6H)

In a fashion similar to the preparation of L^4H, treatment of a diethyl ether (30 mL) solution of 1-aminopiperidine (1.375 mL, 12.74 mmol) and triethylamine (1.776 mL, 12.74 mmol), with acetyl chloride (0.9091 mL, 12.74 mmol) afforded colorless crystals of L^6H after workup (0.227 g, 13%): mp 126–128 °C; IR 1672 (ν_{CO}, s); ^1H NMR ($CDCl_3$, 23 °C, δ) major isomer, 6.49 (br s, 1H, N*H*), 2.69 (t, 4H N(CH_2)$_2$), 2.06 (s, 3H, CH_3), 1.65 (p, 4H, CH_2, 1.38 (p, 4H, CH_2), minor isomer, 6.27 (s, 1H, N*H*), 2.69 (t, 4H, N(CH_2)$_2$), 1.88 (s, 3H, CH_3), 1.65 (p, 4H, CH_2), 1.38 (p, 4H, CH_2); $^{13}C\{^1H\}$($CDCl_3$, 23 °C, ppm) major isomer, 174.00 (s, *C*=O), 57.85 (s, N(*C*H$_2$)$_2$, 25.58 (s, *C*H$_2$), 23.94 (s, *C*H$_2$), minor isomer, 57.21 (s, N(*C*H$_2$)$_2$, 25.17 (s, *C*H$_2$), 22.94 (s, *C*H$_2$), 19.67 (s, *C*H$_3$).

4.8. Preparation of $Cu(L^1)_2$ (**1**)

A 100 mL Schlenk flask, equipped with a magnetic stir bar and a rubber septum, was charged with L^1H (2.102 g, 14.58 mmol) and tetrahydrofuran (50 mL). To this stirred solution at ambient temperature was slowly added potassium hydride (0.614 g, 15.31 mmol) and the resultant colorless solution was stirred for 12 h. This solution was then slowly added over 30 min to a stirred suspension of anhydrous copper(II) chloride (1.000 g, 7.29 mmol) in tetrahydrofuran (40 mL). The resultant purple solution was stirred an additional 30 min at ambient temperature. The volatile components were then removed under reduced pressure and the resultant maroon solid was dissolved in toluene (50 mL). The solution was filtered through a 1-cm pad of Celite on a coarse glass frit, and toluene was then removed under reduced pressure. An analytically pure sample of **1** was obtained as maroon crystals by sublimation at 70 °C/0.05 Torr (1.913 g, 75%): mp 137–139 °C; IR (Nujol, cm^{-1}) 1559 (s), 1515 (m), 1391 (m), 1366 (m), 1358 (m), 1338 (s), 1223 (m), 1206 (s), 1184 (m), 1092 (w), 1028 (w), 1008 (m), 977 (m), 936 (w), 919 (w), 892 (w), 868 (w), 802 (w), 759 (w), 637 (s); ^1H NMR (C_6D_6, 23 °C, δ) 0.81 (s, broad); μ_{eff} = 1.51 and 1.69 BM in the solid state and in benzene solution, respectively. *Anal.* Calc. for $C_{14}H_{30}CuN_4O_2$: C, 48.05; H, 8.64; N, 16.01. Found: C, 48.05; H, 8.42; N, 16.09%.

4.9. Preparation of $Cu(L^2)_2$ (**2**)

In a fashion similar to the preparation of **1**, treatment of anhydrous copper(II) chloride (1.000 g, 7.29 mmol) in tetrahydrofuran (40 mL) with KL^2 (prepared from L^2H (1.898 g, 14.58 mmol) and potassium hydride (0.614 g, 15.31 mmol) in tetrahydrofuran (50 mL)) for a 1 h at ambient temperature afforded **2** (1.197 g, 51%) as maroon crystals after sublimation at 75 °C/0.05 Torr: mp 118–121 °C; IR (Nujol, cm^{-1}) 1677 (m), 1650 (w), 1557 (s), 1420 (m), 1384 (s), 1365 (s), 1354 (s), 1296 (m), 1277 (s), 1235 (m), 1186 (m), 1164 (m), 1119 (m), 1100 (m), 1094 (m), 1011 (m), 985 (s), 959 (m), 928 (m), 890 (w), 837 (m), 783 (w), 742 (m), 637 (s); ^1H NMR (C_6D_6, 23 °C, δ) 14.27 (s, very broad), 0.88 (s, broad); μ_{eff} = 1.69 BM in the solid state. *Anal.* Calc. for $C_{12}H_{26}CuN_4O_2$: C, 44.77; H, 8.14; N, 17.40. Found: C, 45.03; H, 8.02; N, 17.36%.

4.10. Preparation of $Cu(L^3)_2$ (**3**)

In a fashion similar to the preparation of **1**, treatment of anhydrous copper(II) chloride (1.000 g, 7.29 mmol) in tetrahydrofuran (40 mL) with KL^3 (prepared from L^3H (1.489 g, 14.58 mmol) and potassium hydride (0.614 g, 15.31 mmol) in tetrahydrofuran (70 mL)) for 1 h at ambient temperature afforded **3** (0.446 g, 23%) as maroon crystals after sublimation at 80 °C/0.05 Torr: mp 184–187 °C; IR (Nujol, cm^{-1}) 1680 (w), 1654 (m), 1574 (s), 1436 (s), 1423 (s), 1418 (s), 1392 (s), 1329 (s), 1232 (m), 1189 (m), 1167 (w), 1097 (w), 1031 (m), 1012 (m), 994 (s), 928 (m), 868 (w), 789 (w), 669 (s), 648 (s); ^1H NMR (C_6D_6, 23 °C, δ) 12.28 (s, very broad); μ_{eff} = 1.55 BM in the solid state. *Anal.* Calc. for $C_8H_{18}CuN_4O_2$: C, 36.15; H, 6.83; N, 21.08. Found: C, 36.33; H, 6.75; N, 21.07%.

4.11. Preparation of $Co(L^1)_2$ (**4**)

A 100 mL Schlenk flask, equipped with a magnetic stir bar and a rubber septum, was charged with L^1H (2.221 g, 15.40 mmol) and tetrahydrofuran (50 mL). To this stirred solution at ambient temperature was slowly added potassium hydride (0.649 g, 16.17 mmol) and the resultant colorless solution was stirred for 12 h. This solution was then slowly added over 30 min to a stirred suspension of anhydrous cobalt(II) chloride (1.000 g, 7.70 mmol) in tetrahydrofuran (40 mL). The resultant black solution was stirred for 5 h at ambient temperature. The volatile components were then removed under reduced pressure and the resultant black paste was dissolved in toluene (50 mL). The solution was filtered through a 1-cm pad of Celite on a coarse glass frit, and toluene was then removed under reduced pressure. An analytically pure sample of **4** was obtained by sublimation at 75 °C/0.05 Torr to afford red crystals (1.516 g, 57%): mp 137–140 °C; IR (Nujol, cm^{-1}) 1577 (s), 1505 (m), 1416 (w), 1391 (s), 1366 (m), 1359 (m), 1331 (s), 1261 (w), 1223 (m), 1199 (s), 1181 (s), 1091 (m), 1029 (m), 1006 (m), 982 (s), 966 (w), 936 (w), 915 (w), 863 (w), 800 (m), 754 (w), 680 (s); ^1H NMR (C_6D_6, 23 °C, δ) 30.69 (s, very broad), −5.21 (s, broad); μ_{eff} = 2.17 BM in the solid state and benzene solution. *Anal.* Calc. for $C_{14}H_{30}CoN_4O_2$: C, 48.69; H, 8.76; N, 16.22. Found: C, 48.92; H, 8.71; N, 16.36%.

4.12. Preparation of $Cr(L^1)_2$ (**5**)

A 200 mL Schlenk flask, equipped with a magnetic stir bar and a reflux condenser, was charged with anhydrous chromium(II) chloride (1.000 g, 8.14 mmol) and tetrahydrofuran (40 mL). This suspension was refluxed for 1 h. Upon cooling, a solution of KL^1 (prepared from L^1H (2.347 g, 16.27 mmol) and potassium hydride (0.685 g, 17.09 mmol) in tetrahydrofuran (50 mL)) was cannulated slowly into the green suspension over a period of 30 min and the resultant brown solution was stirred for 12 h at ambient temperature. The volatile components were then removed under reduced pressure and the resultant brown solid was dissolved in hexane (60 mL). The solution was filtered through a 1-cm pad of Celite on a coarse glass frit, and orange crystals of **5** formed from the warm concentrated solution upon cooling to room temperature. More crystals of the product were obtained from the concentrated mother liquor at −25 °C (1.708 g, 62%): mp 143–146 °C; IR (Nujol, cm^{-1}) 1562 (s), 1513 (s), 1418 (m), 1391 (s), 1365 (s), 1357 (s), 1335 (s), 1261 (m), 1222 (s), 1202 (s), 1183 (s), 1090 (m), 1028 (m), 1003 (m), 967 (s), 937 (w), 912 (w), 862 (m), 796 (m), 758 (m), 640 (s); ^1H NMR (C_6D_6, 23 °C, δ) 106.51 (s, very broad), 3.64 (s, broad); μ_{eff} = 4.84 and 5.04 BM in solid state and benzene solution, respectively. *Anal.* Calc. for $C_{14}H_{30}CrN_4O_2$: C, 49.69; H, 8.94; N, 16.56. Found: C, 49.87; H, 8.91; N, 16.45%.

4.13. Preparation of $Ni(L^1)_2$ (**6**)

A 100 mL Schlenk flask, equipped with a magnetic stir bar and a rubber septum, was charged with L^1H (1.690 g, 11.72 mmol) and tetrahydrofuran (50 mL). To this stirred solution at ambient temperature was slowly added potassium hydride (0.494 g, 12.31 mmol) and the resultant colorless solution was stirred for 12 h. This solution was then slowly added to a stirred suspension of $NiCl_2{\cdot}CH_3CN$ (1.000 g, 5.86 mmol) in tetrahydrofuran (30 mL). The resultant yellow solution was stirred for 18 h at ambient temperature. The volatile components were then removed under reduced pressure and the resultant yellow solid was dissolved in toluene (50 mL). The solution was filtered through a 1-cm pad of Celite on a coarse glass frit, and toluene was then removed under reduced pressure. An analytically pure sample of **6** was obtained by sublimation at 70 °C/0.05 Torr to afford orange crystals (1.537 g, 76%): mp 140–142 °C; IR (Nujol, cm^{-1}) 1573 (s), 1502 (m), 1415 (m), 1392 (s), 1366 (s), 1359 (m), 1340 (s), 1262 (w), 1223 (m), 1205 (s), 1189 (s), 1091 (w), 1029 (w), 1004 (m), 988 (m), 936 (w), 917 (m), 893 (w), 866 (w), 802 (m), 752 (m), 683 (s); ^1H NMR (C_6D_6, 23 °C, δ) 2.44 (s, 6H, $N(CH_3)_2$), 1.23 (s, 9H, $C(CH_3)_3$); $^{13}C\{^1H\}$ NMR (C_6D_6, 23 °C, ppm) 183.21 (s, C=O), 50.47 (s, $N(CH_3)_2$), 34.45 (s, $C(CH_3)_3$), 28.68 (s, $C(CH_3)_3$). *Anal.* Calc. for

$C_{14}H_{30}N_4NiO_2$: C, 48.72; H, 8.76; N, 16.23. Found: C, 48.90; H, 8.57; N, 16.34%.

4.14. Preparation of $Ni(L^2)_2$ (**7**)

In a fashion similar to the preparation of **6**, treatment of $NiCl_2{\cdot}CH_3CN$ (1.000 g, 5.86 mmol) in tetrahydrofuran (30 mL) with KL^2 (prepared from L^2H (1.526 g, 11.72 mmol) and potassium hydride (0.494 g, 12.31 mmol) in tetrahydrofuran (50 mL)) for a 18 h at ambient temperature afforded **7** (1.152 g, 62%) as orange crystals upon sublimation at 80 °C/0.05 Torr: mp 125–128 °C; IR (Nujol, cm^{-1}) 1578 (s), 1495 (m), 1416 (m), 1358 (s), 1348 (s), 1308 (m), 1291 (s), 1232 (m), 1195 (m), 1181 (m), 1165 (w), 1103 (w), 1071 (s), 1005 (m), 993 (s), 919 (m), 897 (w), 821 (w), 749 (m), 725 (s); ^1H NMR (C_6D_6, 23 °C, δ) 2.48 (s, 6H, $N(CH_3)_2$), 2.44 (septet, 1H, $CH(CH_3)_2$), 1.12 (d, 6H, $CH(CH_3)_2$); $^{13}C\{^1H\}$ NMR (C_6D_6, 23 °C, ppm) 181.30 (s, C=O), 50.52 (s, $N(CH_3)_2$), 30.04 (s, $CH(CH_3)_2$), 20.58 (s, $CH(CH_3)_2$). *Anal.* Calc. for $C_{12}H_{26}N_4NiO_2$: C, 45.46; H, 8.27; N, 17.67. Found: C, 45.59; H, 8.23; N, 17.61%.

4.15. Preparation of $Ni(L^3)_2$ (**8**)

In a fashion similar to the preparation of **6**, treatment of $NiCl_2{\cdot}CH_3CN$ (0.835 g, 4.895 mmol) in tetrahydrofuran (30 mL) with KL^3 (prepared from L^3H (1.000 g, 9.791 mmol) and potassium hydride (0.401 g, 10.000 mmol) in tetrahydrofuran (50 mL)) for 18 h at ambient temperature afforded **8** (0.792 g, 62%) as orange crystals upon sublimation at 80 °C/0.05 Torr: mp 164–166 °C; IR (Nujol, cm^{-1}) 1586 (s), 1337 (s), 1291 (s), 1232 (m), 1195 (m), 1178 (m), 1104 (w), 1041 (w), 1032 (w), 995 (s), 919 (m), 891 (w), 865 (w), 770 (m), 711 (s), 642 (s); ^1H NMR (C_6D_6, 23 °C, δ) 2.50 (s, 6H, $N(CH_3)_2$), 1.70 (s, 3H, $CO(CH_3)$); $^{13}C\{^1H\}$ NMR (C_6D_6, 23 °C, ppm) 175.00 (s, C=O), 50.51 (s, $N(CH_3)_2$), 20.58 (s, $COCH_3$). *Anal.* Calc. for $C_8H_{18}N_4NiO_2$: C, 36.82; H, 6.95; N, 21.47. Found: C, 37.17; H, 7.04; N, 21.19%.

4.16. Preparation of $Ni(L^4)_2$ (**9**)

A 100 mL Schlenk flask, equipped with a magnetic stir bar and rubber septum, was charged with L^4H (1.000 g, 5.43 mmol) and tetrahydrofuran (20 mL). To this stirred solution at ambient temperature was slowly added potassium hydride (0.218 g, 5.50 mmol) and the resultant colorless solution was stirred for 2 h. This was then slowly added to a stirred suspension of $NiCl_2{\cdot}CH_3CN$ (0.463 g, 2.715 mmol) in tetrahydrofuran (30 mL). The resultant orange solution was stirred for 17 h at ambient temperature. The volatile components were then removed under reduced pressure and the resultant orange solid was dissolved in toluene (35 mL). The solution was filtered through a 1-cm pad of Celite on a coarse glass frit, and the toluene was then removed under reduced pressure. An analytically pure sample of **9** was obtained by sublimation at 155 °C/0.05 Torr as orange crystals (0.294 g, 13%): mp 203–205 °C; IR (Nujol, cm^{-1}) 1575 (s), 1357 (s), 1339 (s), 1203 (s), 1166 (m), 1178 (m), 1072 (w), 1044 (w), 1027 (w), 970 (m), 951 (m), 890 (w), 871 (w), 850 (w), 793 (m), 750 (w), 684 (s); ^1H NMR (C_6D_6, 23 °C, δ) 3.42 (d, 4H, $N(CH_2)_2$), 3.05 (m, 4H, CH_2), 2.21 (m, 4H, CH_2), 1.30 (s, 9H, $C(CH_3)_3$); $^{13}C\{^1H\}$ NMR (C_6D_6, 23 °C, ppm) 180.64 (s, C=O), 58.35 (s, $N(CH_2)_2$), 28.77 (s, $C(CH_3)_3$), 24.17 (s, CH_2), 20.29 (s, CH_2). *Anal.* Calc. for $C_{20}H_{38}N_4NiO_2$: C, 56.49; H, 9.01; N, 13.18. Found: C, 56.81; H, 8.71; N, 13.13%.

4.17. Preparation of $Ni(L^5)_2$ (**10**)

In a fashion similar to the preparation of **9**, treatment of $NiCl_2{\cdot}CH_3CN$ (0.596 g, 3.49 mmol) in tetrahydrofuran (25 mL) with KL^5 (prepared from L^5H (1.188 g, 6.98 mmol) and potassium hydride (0.285, 7.05 mmol) in tetrahydrofuran (30 mL)) for 17 h at ambient temperature afforded **10** (0.304 g, 11%) as orange crystals from sublimation at 110 °C/0.05 Torr: mp 115–117 °C; IR (Nujol, cm^{-1}) 1583 (s), 1349 (s), 1270 (s), 1205 (w), 1166 (m), 1178 (m), 1080 (s), 1046 (w), 1028 (w), 977 (m), 948 (m), 860 (m); ^1H NMR (C_6D_6, 23 °C, δ) 3.50 (m, 4H, CH_2), 3.07 (m, 4H, CH_2), 2.57 (septet, 1H, $CH(CH_3)_2$), 2.24 (m, 2H, CH_2), 1.20 (d, 6H, $CH(CH_3)_2$); $^{13}C\{^1H\}$(C_6D_6, 23 °C, ppm) 180.70 (s, C=O), 58.36 (s, $N(CH_2)_2$), 30.31 (s, $CH(CH_3)_2$), 24.16 (s, CH_2), 20.79 (s, CH_2), 20.34 (s, CH_2). *Anal.* Calc. for $C_{18}H_{34}N_4NiO_2$: C, 54.43; H, 8.63; N, 14.11. Found: C, 54.27; H, 8.71; N, 13.92%.

4.18. Preparation of $Ni(L^6)_2$ (**11**)

In a fashion similar to the preparation of **9**, treatment of $NiCl_2{\cdot}CH_3CN$ (0.618 g, 3.62 mmol) in tetrahydrofuran (30 mL) with KL^6 (prepared from L^6H (1.029 g, 7.24 mmol) and potassium hydride (0.295, 7.35 mmol) in tetrahydrofuran (25 mL)) for 17 h at ambient temperature afforded **11** (0.723 g, 29%) as orange crystals from sublimation at 150 °C/0.05 Torr: mp 230–232 °C; IR (Nujol, cm^{-1}) 1591 (s), 1325 (s), 1302 (s), 1200 (s), 1159 (m), 1159 (m), 1073 (w), 1046 (w), 1017 (w), 982 (m), 945 (m), 875 (m), 844 (m), 770 (w), 711 (s), 662 (w), 636 (m); ^1H NMR (C_6D_6, 23 °C, δ) 3.57 (d, 4H, $N(CH_2)_2$), 3.06 (m, 2H, CH_2), 2.34 (m, 2H, CH_2), 1.83 (s, 3H, CH_3); $^{13}C\{^1H\}$ NMR (C_6D_6, 23 °C, ppm) 174.47 (s, C=O), 58.13 (s, $N(CH_2)_2$), 24.03 (s, CH_2), 20.25 (s, CH_2), 16.67 (s, $COCH_3$). *Anal.* Calc. for $C_{14}H_{26}N_4NiO_2$: C, 49.30; H, 7.68; N, 16.43. Found: C, 49.19; H, 7.78; N, 16.45%.

4.19. Preparation of $[Fe(L^1)_2]_2$ (**12**)

A 100 mL Schlenk flask, equipped with a magnetic stir bar and a rubber septum, was charged with L^1H (1.051 g, 7.29 mmol) and tetrahydrofuran (25 mL). To this stirred solution at ambient temperature was slowly added potassium hydride (0.307 g, 7.66 mmol) and the resultant colorless solution was stirred for 12 h. This solution was then slowly added over 30 min to a stirred suspension of anhydrous iron(II) chloride (0.464 g, 3.64 mmol) in tetrahydrofuran (20 mL). The resultant pale blue solution was stirred for 3 h and the volatile components were then removed under reduced pressure. The resultant pale blue paste was dissolved in hexane (50 mL) and the pale green solution was filtered through a 1-cm pad of Celite on a coarse glass frit. Hexane was then removed under reduced pressure to afford **12** as a gray solid (1.084 g, 87%). Pale green crystals of **12** suitable for single crystal X-ray crystallographic analysis were obtained by slow crystallization at −23 °C in hexane (0.349 g, 28%): mp 155–157 °C; IR (Nujol, cm^{-1}); 1719 (w), 1632 (s), 1563 (s), 1554(s), 1523 (s), 1351 (s), 1340 (s), 1313 (m), 1262 (w), 1227 (w), 1210 (s), 1171 (s), 1090 (w), 1026 (w), 1009 (m), 963 (s), 860 (m), 608 (m); μ_{eff} = 7.99 and 4.55 BM in solid state and benzene solution, respectively. *Anal.* Calc. for $C_{28}H_{60}Fe_2N_8O_4$: C, 49.13; H, 8.83; N, 16.37. Found: C, 51.75; H, 9.37; N, 16.63%.

4.20. Preparation of $[Mn(L^1)_2]_2$ (**13**)

A 100 mL Schlenk flask, equipped with a magnetic stir bar and a rubber septum, was charged with anhydrous manganese(II) bromide (0.791 g, 3.64 mmol) and tetrahydrofuran (20 mL). To this stirred suspension at ambient temperature was slowly added KL^1 (prepared from L^1H (1.051 g, 7.29 mmol) and potassium hydride (0.307 g, 7.66 mmol) in tetrahydrofuran (25 mL)). The resultant suspension was stirred for 18 h and the volatile components were then removed under reduced pressure. The resultant solid was dissolved in toluene (50 mL) and filtered through a 1-cm pad of Celite

on a coarse glass frit. Toluene was then removed under reduced pressure to afford **13** as a pale brown solid (1.093 g, 88%). Colorless crystals of **13** suitable for X-ray crystallographic analysis were obtained from a concentrated solution in toluene at −25 °C (0.149 g, 12%): mp 92–94 °C; IR (Nujol, cm^{-1}) 1563 (s), 1550 (s), 1521 (m), 1513 (m), 1391 (m), 1366 (s), 1353 (m), 1338 (s), 1316 (s), 1262 (w), 1211 (s), 1192 (m), 1176 (s), 1092 (w), 1030 (w), 1010 (m), 964 (m), 928 (w), 892 (w), 860 (w), 794 (w), 758 (w); ^1H NMR (C_6D_6, 23 °C, δ) 5.54 (s, broad); μ_{eff} = 9.62 and 5.47 BM in solid state and in benzene solution, respectively. *Anal.* Calc. for $C_{28}H_{60}Mn_2N_8O_4$: C, 49.26; H, 8.86; N, 16.41. Found: C, 50.61; H, 8.78; N, 16.62%.

*4.21. X-ray crystallographic structure determinations of **1**, **4**, **5**, **6**, and **12***

Diffraction data were measured on a Bruker X8 APEX-II kappa geometry diffractometer with Mo radiation and a graphite monochromator. Frames were collected at 100 K with the detector at 40 mm and 0.3–0.5° between each frame. The frames were recorded for 3–5 s. APEX-II [47] and SHELX [48] software were used in the collection and refinement of the models. All structures contained discrete neutral complexes without ions or solvent.

Acknowledgments

We are grateful to the U.S. National Science Foundation (Grant No. CHE-0910475) and SAFC Hitech for support of this research.

Appendix A. Supplementary data

CCDC 878262–878266 contain the supplementary crystallographic data for **1**, **4**, **5**, **6**, and **12**. These data can be obtained free of charge via http://www.ccdc.cam.ac.uk/conts/retrieving.html, or from the Cambridge Crystallographic Data Centre, 12 Union Road, Cambridge CB2 1EZ, UK; fax: (+44) 1223-336-033; or e-mail: deposit@ccdc.cam.ac.uk.

References

[1] A. Roule, M. Amuntencei, E. Deronzier, P.H. Haumesser, S. Da Silva, X. Avale, O. Pollet, R. Baskaran, G. Passemard, Microelectron. Eng. 84 (2007) 2610.
[2] (a) C.H. Winter, Aldrichim. Acta (2000) 3;
(b) Y.S. Won, Y.S. Kim, T.J. Anderson, L.L. Reitfort, I. Ghiviriga, L. McElwee-White, J. Am. Chem. Soc. 128 (2006) 13781;
(c) L. McElwee-White, Dalton Trans. (2006) 5327;
(d) W. Koh, D. Kumar, W.-M. Li, H. Sprey, I.J. Raaijmakers, Solid State Technol. 48 (2005) 54;
(e) H.S. Sim, S.-I. Kim, Y.T. Kim, J. Vac. Sci. Technol., B 21 (2003) 1411;
(f) B.H. Lee, K. Yong, J. Vac. Sci. Technol., B 22 (2004) 2375.
[3] International Technology Roadmap for Semiconductors, http://www.itrs.net/.
[4] (a) M. Haneda, J. Iijima, J. Koike, Appl. Phys. Lett. 90 (2007) 252107;
(b) T. Usui, H. Nasu, S. Takahashi, N. Shimizu, T. Nishikawa, M. Yoshimaru, H. Shibata, M. Wada, J. Koike, IEEE Trans. Electron. Dev. 52 (2006) 2492;
(c) J. Koike, M. Wada, Appl. Phys. Lett. 87 (2005) 041911;
(d) J. Iijima, Y. Fujii, K. Neishi, J. Koike, J. Vac. Sci. Technol., B 27 (2009) 1963;
(e) S.-M. Chung, J. Koike, J. Vac. Sci. Technol., B 27 (2009) L28;
(f) Y. Otsuka, J. Koike, H. Sako, K. Ishibashi, N. Kawasaki, S.M. Chung, I. Tanaka, Appl. Phys. Lett. 96 (2010) 012101;
(g) G.S. Chen, S.T. Chen, Y.L. Lu, Electrochem. Commun. 12 (2010) 1483;
(h) J.G. Lozano, S. Lozano-Perez, J. Bogan, Y.C. Wang, B. Brennan, P.D. Nellist, G. Hughes, Appl. Phys. Lett. 98 (2011) 123112;
(i) P. Casey, J. Bogan, B. Brennan, G. Hughes, Appl. Phys. Lett. 98 (2011) 113508;
(j) H. Au, Y. Lin, H. Kim, E. Beh, Y. Liu, R.G. Gordon, J. Electrochem. Soc. 157 (2010) D341;
(k) H. Au, Y. Lin, R.G. Gordon, J. Electrochem. Soc. 158 (2011) D248;
(l) V.K. Dixit, K. Neishi, N. Akao, J. Koike, IEEE Trans. Dev. Mater. Reliab. 11 (2011) 295.
[5] J.P. Chu, C.H. Lin, V.S. John, Appl. Phys. Lett. 91 (2007) 132109.
[6] K. Barmak, C. Cabral Jr., K.P. Rodbell, J.M.E. Harper, J. Vac. Sci. Technol., B 24 (2006) 2485.
[7] (a) S.H. Kang, JOM 60 (2008) 28;
(b) C.A.F. Vaz, J.A.C. Bland, G. Lauhoff, Rep. Prog. Phys. 71 (2008) 056501;
(c) Y. Shiratsuchi, M. Yamamoto, S.D. Bader, Prog. Surf. Sci. 82 (2007) 121.
[8] C.-S. Chen, J.-H. Lin, T.-W. Lai, Chem. Commun. (2008) 4983.
[9] (a) H.-B.-R. Lee, S.-H. Band, W.-H. Kim, G.H. Gu, Y.K. Lee, T.-M. Chung, C.G. Kim, C.G. Park, H. Kim, Jpn. J. Appl. Phys. 49 (2010) 05FA11;
(b) H.-B.-R. Lee, G.H. Gu, J.Y. Son, C.G. Park, H. Kim, Small 4 (2008) 2247;
(c) C.-M. Yang, S.-W. Yun, J.-B. Ha, K.-I. Na, H.-I. Cho, H.-B. Lee, J.-H. Jeong, S.-H. Kong, S.-H. Hahm, J.-H. Lee, Jpn. J. Appl. Phys. 46 (2007) 1981;
(d) K.-W. Do, C.-M. Yang, I.-S. Kang, K.-M. Kim, K.-H. Back, H.-I. Cho, H.-B. Lee, S.-H. Kong, S.-H. Hahm, D.-H. Kwon, J.-H. Lee, J.H. Lee, Jpn. J. Appl. Phys. 45 (2006) 2975;
(e) J. Chae, H.-S. Park, S.-W. Kang, Electrochem. Solid State Lett. 5 (2002) C64.
[10] (a) H. Kim, Surf. Coat. Technol. 200 (2006) 3104;
(b) H. Kim, J. Vac. Sci. Technol., B 21 (2003) 2231;
(c) S.M. Merchant, S.H. Kang, M. Sanganeria, B. van Schravendijk, T. Mountsier, JOM – J. Miner. Met. Mater. Soc. 52 (2001) 43;
(d) S.-Q. Wang, MRS Bull. 19 (1994) 30.
[11] (a) M. Leskelä, M. Ritala, Angew. Chem., Int. Ed. 42 (2003) 5548;
(b) M. Leskelä, M. Ritala, Thin Solid Films 409 (2002) 138;
(c) M. Ritala, M. Leskelä, Nanotechnology 10 (1999) 19;
(d) L. Niinistö, Curr. Opin. Solid State Mater. Sci. 3 (1998) 147;
(e) M. Ritala, Appl. Surf. Sci. 112 (1997) 223;
(f) T. Suntola, Thin Solid Films 216 (1992) 84;
(g) M. Putkonen, L. Niinistö, Top. Organomet. Chem. 9 (2005) 125.
[12] (a) V. Vidjayacoumar, D.J.H. Emslie, S.B. Clendenning, J.M. Blackwell, J.F. Britten, A. Rheingold, Chem. Mater. 22 (2010) 4844;
(b) V. Vidjayacoumar, D.J.H. Emslie, J.M. Blackwell, S.B. Clendenning, J.F. Britten, Chem. Mater. 22 (2010) 4854.
[13] H.B. Profijt, S.E. Potts, M.C.M. van de Sanden, W.M.M. Kessels, J. Vac. Sci. Technol., A 25 (2011) 050801.
[14] B.H. Lee, J.K. Hwang, J.W. Nam, S.U. Lee, J.T. Kim, S.-M. Koo, A. Baunemann, R.A. Fischer, M.M. Sung, Angew. Chem., Int. Ed. 48 (2009) 4536.
[15] I.J. Hsu, B.E. McCandless, C. Weiland, B.G. Willis, J. Vac. Sci. Technol., A 27 (2009) 660.
[16] B.S. Lim, A. Rahtu, R.G. Gordon, Nat. Mater. 2 (2003) 748.
[17] Z. Li, A. Rahtu, R.G. Gordon, J. Electrochem. Soc. 153 (2006) C787.
[18] Z. Li, R.G. Gordon, D.B. Farmer, Y. Lin, J. Vlassak, Electrochem. Solid State Lett. 8 (2005) G182.
[19] R. Solanki, B. Pathangey, Electrochem. Solid State Lett. 3 (2000) 479.
[20] P. Mårtensson, J.-O. Carlsson, Chem. Vap. Deposition 3 (1997) 45.
[21] M. Juppo, M. Ritala, M. Leskelä, J. Vac. Sci. Technol., A 15 (1997) 2330.
[22] K.-H. Park, A.Z. Bradley, J.S. Thompson, W.J. Marshall, Inorg. Chem. 45 (2006) 8480.
[23] J.S. Thompson, L. Zhang, J.P. Wyre, D.J. Brill, K.G. Lloyd, Thin Solid Films 517 (2009) 2845.
[24] J. Huo, R. Solanki, J. Mater. Res. 17 (2002) 2394.
[25] Z. Li, R.G. Gordon, Chem. Vap. Deposition 12 (2006) 435.
[26] T. Waechtler, S.-F. Ding, L. Hofmann, R. Mothes, Q. Xie, S. Oswald, C. Detavernier, S.E. Schulz, X.-P. Qu, H. Lang, T. Gessner, Microelectron. Eng. 88 (2011) 684.
[27] A. Niskanen, A. Rahtu, T. Sajavaara, K. Arstila, M. Ritala, M. Leskelä, J. Electrochem. Soc. 152 (2005) G25.
[28] D.-Y. Moon, D.-S. Han, S.-Y. Shin, J.-W. Park, B.M. Kim, J.H. Kim, Thin Solid Films 519 (2011) 3636.
[29] T.J. Knisley, T.C. Ariyasena, T. Sajavaara, M.J. Saly, C.H. Winter, Chem. Mater. 23 (2011) 4417.
[30] (a) J. Kwon, M. Saly, M.D. Halls, R.K. Kanjolia, Y.J. Chabal, Chem. Mater. 24 (2012) 1025;
(b) J.-M. Kim, H.-B.-R. Lee, C. Lansalot, C. Dussarrat, J. Gatineau, H. Kim, Jpn. J. Appl. Phys. 49 (2010) 05FA10;
(c) Z. Li, D.K. Lee, M. Coulter, L.N.J. Rodriguez, R.G. Gordon, Dalton Trans. (2008) 2592;
(d) H.-B.-R. Lee, H. Kim, ECS Trans. 16 (2008) 219;
(e) K. Kim, K. Lee, S. Han, T. Park, Y. Lee, J. Kim, S. Yeom, H. Jeon, Jpn. J. Appl. Phys. 46 (2007) L173;
(f) K. Lee, K. Kim, T. Park, H. Jeon, Y. Lee, J. Kim, S. Yeom, J. Electrochem. Soc. 154 (2007) H899;
(g) K. Kim, K. Lee, S. Han, W. Jeong, H. Jeon, J. Electrochem. Soc. 154 (2007) H177;
(h) H.-B.-R. Lee, H. Kim, Electrochem. Solid State Lett. 9 (2006) G323.
[31] S.O. Kucheyev, J. Biener, T.F. Baumann, Y.M. Wang, A.V. Hamza, Z. Li, D.K. Lee, R.G. Gordon, Langmuir 24 (2008) 943.
[32] D.-Y. Moon, D.-S. Han, J.-H. Park, S.-Y. Shin, J.-W. Park, B.M. Kim, J.Y. Cho, Thin Solid Films (2012), http://dx.doi.org/10.1016/j.tsf.2012.02.015.
[33] (a) D. Kost, I. Kalikhman, Acc. Chem. Res. 42 (2009) 303;
(b) I. Kalikhman, E. Kertsnus-Banchik, B. Gostevskii, N. Kocher, D. Stalke, D. Kost, Organometallics 28 (2009) 512;
(c) V. Jouikov, B. Gostevskii, I. Kalikhman, D. Kost, Organometallics 26 (2007) 5791;
(d) B. Gostevskii, G. Silvert, K. Adear, A. Sivaramakrishna, D. Stalke, S. Deuerlein, N. Kocher, M.G. Voronkov, I. Kalikhman, D. Kost, Organometallics 24 (2005) 2913;
(e) I. Kalikhman, V. Kingston, B. Gostevskii, V. Pestunovich, D. Stalke, B. Walfort, D. Kost, Organometallics 21 (2002) 4468;
(f) D. Kost, I. Kalikhman, M. Raban, J. Am. Chem. Soc. 117 (1995) 11512.

[34] S. Yakubovich, I. Kalikhman, D. Kost, Dalton Trans. 39 (2010) 9241.
[35] (a) V.Y. Gusev, A.V. Radushev, P.A. Slepukhin, Z.A. Vnutskikh, Russ. J. Inorg. Chem. 53 (2008) 83;
(b) V.F. Shulgin, N.S. Pevzner, V.Y. Zub, N.G. Strizhakova, Y.A. Maletin, Inorg. Chem. Commun. 4 (2001) 134.
[36] J.M. Hoover, A. DiPasquale, J.M. Mayer, F.E. Michael, J. Am. Chem. Soc. 132 (2010) 5043.
[37] W.M. Haynes (Ed.), Handbook of Chemistry and Physics, 92nd ed., CRC Press, Boca Raton, Florida, 2012. p. 9048.
[38] J.T. Pulkkinen, R. Laatikainen, M.J. Ahlgrén, M. Peräkylä, J.J. Vepsäläinen, J. Chem. Soc., Perkin Trans. 2 (2000) 777.
[39] X. He, Y. Yao, X. Luo, J. Zhang, Y. Liu, L. Zhang, Q. Wu, Organometallics 22 (2003) 4952.
[40] W.H. Monillas, G.P.A. Yap, K.H. Theopold, J. Chem. Crystallogr. 39 (2009) 380.
[41] A.W. Addison, T.N. Rao, J. Reedijk, J.V. Rijn, G.C. Verschoor, J. Chem. Soc., Dalton Trans. (1984) 1349.
[42] S.C. Goel, K.S. Kramer, M.Y. Chiang, W.E. Buhro, Polyhedron 9 (1990) 611.
[43] J. Reedijk, W.J. Marshall, Recl. Trav. Chim. Pays-Bas 87 (1968) 552.
[44] D.F. Evans, J. Chem. Soc. (1959) 2003.
[45] T.A. Sokolova, L.A. Ovsyannikova, N.P. Zapevalova, Zh. Obshch. Khim. 2 (1966) 818.
[46] R.L. Hinman, J. Am. Chem. Soc. 78 (1956) 1645.
[47] APEX II collection and processing programs are distributed by the manufacturer, Bruker AXS Inc., Madison, WI, USA, 2009.
[48] G.M. Sheldrick, Acta Crystallogr., Sect. A 64 (2008) 112.